

High-Resolution Ultrasound for Diagnostic Assessment of the Great Auricular Nerve – Normal and First Pathologic Findings

Hochauflösender Ultraschall in der Diagnostik des N. auricularis magnus – Normalbefund und erste pathologische Befunde

Authors

D. Lieba-Samal¹, C. Pivec², H. Platzgummer², G. M. Gruber³, S. Seidel¹, M. Bernathova², G. Bodner², T. Moritz²

Affiliations

¹ Neurology, Medical University of Vienna, Austria

² Biomedical Imaging and Image-guided Therapy, Medical University of Vienna, Austria

³ Systematic Anatomy, Medical University of Vienna, Austria

Key words

- head/neck
- ear
- great auricular nerve
- neuroma
- neuropathic pain

received 31.10.2013

accepted 19.2.2014

Bibliography

DOI <http://dx.doi.org/10.1055/s-0034-1366354>
 Published online: May 13, 2014
 Ultraschall in Med 2015; 36:
 342–347 © Georg Thieme
 Verlag KG Stuttgart · New York ·
 ISSN 0172-4614

Correspondence

Dr. Doris Lieba-Samal
 Neurology, Medical University
 of Vienna
 Währinger Gürtel 18–20
 1090 Vienna
 Austria
 Tel.: ++43/1/4 04 00 31 17
 Fax: ++43/1/4 04 00 31 41
 doris.lieba-samal@
 meduniwien.ac.at

Abstract



Purpose: The great auricular nerve (GAN) is a sensory branch of the superficial cervical plexus. While its blockade is an established procedure, little is known about the ultrasound appearance of pathologic conditions of the GAN itself. We, therefore, aimed to evaluate the possibility of the visualization and diagnostic assessment of the GAN along its entire course by means of high-resolution ultrasound (HRUS).

Materials and Methods: To assess the feasibility of visualization, we performed HRUS with an 18 MHz probe, HRUS-guided, fine-needle ink markings and consecutive dissection in six anatomical specimens. Then, we measured the diameter of the GAN in healthy volunteers and finally performed a retrospective review of patients referred for HRUS examinations because of pain within GAN territory between August 1, 2012 and August 1, 2013.

Results: The GAN was clearly visible with HRUS from its formation to the final branches, and was marked successfully on both sides in all anatomical specimens (n = 12). The mean average in-vivo was 0.14 cm ± 0.03 (range 0.08 – 0.2). Seven cases of patients with GAN pathologies of various origins (idiopathic, traumatic, tumorous and iatrogenic) were identified, of which 6 were visible on HRUS and all of which could be confirmed by complete resolution of symptoms after selective HRUS-guided GAN block.

Conclusion: This study confirms the reliable ability to visualize the GAN with HRUS throughout its course, both in anatomical specimens and in vivo. The provided cases show that pathologies of the GAN seem to have a variety of causes and may not be rare. We, therefore, encourage the use of HRUS in patients with unclear pain in the auricular, periauricular and posterior-lateral head.

Zusammenfassung



Ziel: Der Nervus auricularis magnus (GAN) ist ein sensibler Ast des Plexus cervicalis superficialis. Während seine Blockade eine etablierte Methode ist, ist wenig bekannt über die sonografische Darstellung pathologischer Zustände des GAN selbst. Ziel dieser Studie war es, Visualisierbarkeit und diagnostisches Potential des hochauflösenden Ultraschalls (HRUS) im gesamten Verlauf des GAN zu evaluieren.

Material und Methoden: Zur Klärung der Visualisierbarkeit wurde eine HRUS-gezielte Markierung der GAN und anschließende Sektion in sechs anatomischen Präparaten durchgeführt. Danach wurde der Durchmesser des GANs bei 10 gesunden ProbandInnen vermessen. Zusätzlich erfolgte eine retrospektive Analyse der PatientInnen, die zwischen 1. August 2012 und 1. August 2013 aufgrund von Schmerzen im Bereich des GAN untersucht wurden.

Ergebnisse: Der GAN konnte von seiner Formierung bis in die Endäste verfolgt werden und wurde in allen anatomischen Präparaten erfolgreich markiert (n = 12). Der mittlere Durchmesser in-vivo war 0,14 cm ± 0,03 (0,08 – 0,2 cm). Sieben PatientInnen mit GAN-Pathologien unterschiedlicher Genese wurden identifiziert (idiopathisch, traumatisch, tumor-assoziiert und iatrogen), von denen 6 mittels HRUS visualisiert werden konnten und alle durch vollständige Remission der Schmerzen nach HRUS-gezielter, selektiver Blockade des GAN bestätigt werden konnten.

Schlussfolgerungen: Diese Studie bestätigt die Visualisierbarkeit des GAN sowohl im anatomischen Präparat als auch in vivo. Die präsentierten Fälle zeigen, dass das breite Spektrum möglicher Pathologien des GAN wesentlich häufiger sein könnte als angenommen. Wir empfehlen eine HRUS-Abklärung bei PatientInnen mit Schmerzen im Bereich des Ohres, periaurikulär und posterolateralen Kopfes.

Introduction

The superficial cervical plexus lies beneath the M. sternocleidomastoideus, between the Mm. scaleni and the M. levator scapulae. It receives fibers from the C2 and C3 ventral roots, which ultimately form the sensory cutaneous nerves including the minor occipital nerve (C2, C3), the transverse cervical nerve (C2, C3), the great auricular nerve (GAN) (C2, C3) and the supraclavicular nerves (C3, C4). These nerves usually perforate the lateral superficial cervical fascia together at Erb's point, i. e. at the crossing of the posterior margins of the platysma and the sternocleidomastoid muscle and run onward subcutaneously [1, 2].

The GAN turns cranially, splits into an anterior and posterior branch in the majority of cases and supplies the skin of the outer ear, and the skin posterior to the mastoid process, above the auricle and ventrally the skin over the parotid gland (► Fig. 1) [1, 3]. To date, the GAN has been of importance for surgery that involves the parotid gland or the neck, where its preservation offers a more beneficial outcome [4, 5], or for blockades in the case of surgical procedures or pain conditions [6–8].

Reports on GAN neuropathy are rare and most of these deal with its involvement in leprosy, where thickening of the GAN and neuropathic pain in its territory can be the sole symptoms [9–11]. Occasionally, there are reports of iatrogenic injury caused by inappropriate positioning during surgery [12, 13]. One case report describes a patient with a chronic daily migrainous headache, starting after endolymphatic shunt surgery.

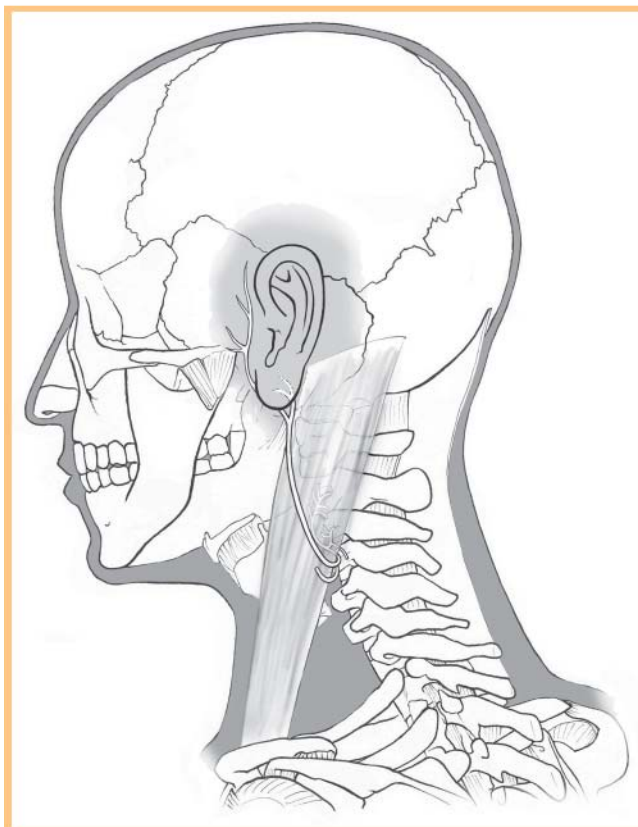


Fig. 1 Illustration showing the course of the GAN. With kind permission from Jeanette Schulz.

Abb. 1 Illustration des Verlaufs des GAN. Mit freundlicher Genehmigung von Jeanette Schulz

Surgical exploration revealed traumatic neuromas of the GAN and the minor occipital nerve. Resection of the neuromas yielded complete symptom relief [14].

To date, evaluation of the GAN has been restricted to diagnostic blockade based on landmarks. However, this has been hindered by the large variability of its course [1, 15]. Recently, an ultrasound-guided infiltration technique was described [16, 17]. However, high-resolution ultrasound (HRUS) is expected to offer possibilities beyond that: the diagnostic assessment of pathologies and subsequent targeted therapy. As this was described for the greater occipital nerve [18] and other small nerves of the neck [19], which can be assumed to have a comparable diameter, we hypothesized that GAN pathologies could also be visible with HRUS.

This study, therefore, aimed at: first, confirming the correct identification of the GAN by HRUS with ink marking and consecutive dissection in anatomical specimens; second, providing first measurements of GAN diameter in healthy volunteers and third, the presentation of cases with GAN pathology as found with HRUS.

Methods

Technique of ultrasound examination

HRUS examinations were performed using a GE Logic E9 ultrasound platform with high-frequency probes (GE ML 6–15-D, L 8–18i-D). All examinations were performed by examiners experienced in peripheral nerve ultrasound, following a standardized assessment protocol, which started at the posterior border of the sternocleidomastoid muscle. The probe was moved cranially and caudally in the transverse view until a structure was identified beneath the sternocleidomastoid muscle, which was positioned around its posterior border and ran cranially onward – which was presumed to be the GAN. After identification, the nerve was examined both proximally at the formation of the superficial cervical plexus as well as distally, following its course up to the division of the final branches. An example of a normal finding with positioning of the ultrasound probe is depicted in ► Fig. 2.

The study was approved by the local ethics committee.



Fig. 2 Probe positioning and normal finding of the GAN (white arrows) in HRUS with the nerve below and above the sternocleidomastoid muscle.

Abb. 2 Sondenhaltung und Normalbefund des GAN (weiße Pfeile) im HRUS mit dem Nerven ober- und unterhalb des Musculus sternocleidomastoideus (SCM).

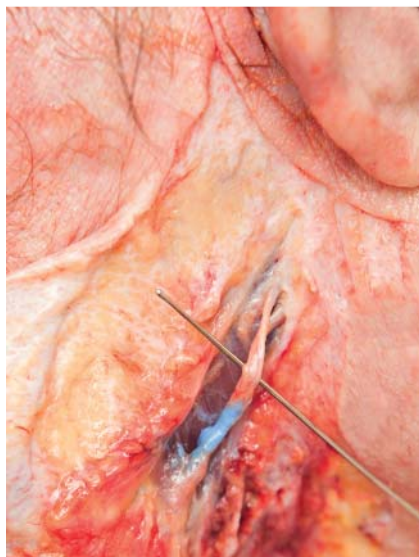


Fig. 3 Example of finding after dissection showing intraneural ink marking of the GAN.

Abb. 3 Beispiel eines Befundes nach Sektion mit intraneuraler Tintemarkierung des GAN.

Table 1 Measurements of GAN diameter in 10 healthy volunteers (given in cm).

no.	gender	age	right GAN	left GAN
1	F	41	0.18	0.15
2	F	36	0.15	0.15
3	F	46	0.18	0.17
4	M	53	0.11	0.14
5	M	47	0.13	0.16
6	F	48	0.14	0.12
7	F	42	0.10	0.08
8	M	33	0.19	0.20
9	M	34	0.12	0.15
10	F	22	0.11	0.12

Ultrasound in an anatomic specimen

After six randomly selected anatomic specimens in legal custody of the Department of Systematic Anatomy, Medical University of Vienna were received, HRUS was performed as described above. After locating the GAN, a small amount of blue dye (0.1 ml) mixed with latex was injected adjacent to the nerve. Anatomical dissection was performed to confirm the exact location of US-guided dye injection.

Ultrasound in healthy volunteers

Healthy volunteers were recruited via notice at the department and word-of-mouth acquisition. After written informed consent was given, the GAN was assessed on both sides and measurement of the diameter was carried out beneath the sternocleidomastoid muscle, as it is usually a single nerve trunk there, while the point of splitting into the anterior and posterior branch varies interindividually.

Ultrasound in patients

Between August 1, 2012 and August 1, 2013 we monitored seven patients who were referred to the Department of Biomedical Imaging and Image-Guided Therapy, and in whom GAN pathology was detected with HRUS. For confirmation of the causative relationship between GAN pathology and pain, selective HRUS-guided diagnostic blockade on transverse scan with in-plane technique of the GAN was performed in all patients with 0.3 ml of local anesthetic. The point of blockade was chosen proximally to the suspected lesion, i.e., the point where the GAN winds around the posterior border of the sternocleidomastoid muscle in most cases.

Results

The GAN was clearly visible within all anatomical specimens, all volunteers and in all patients.

Table 2 Summary of patient histories and HRUS findings of those cases identified at our department.

no.	gender	age	history	HRUS findings	diagnosis
1	F	63	after bilateral neck dissection, the patient developed pain in the lateral head and neck on the left side	enlarged GAN on the symptomatic side, which was discontinued within the scar tissue	entrapment of the GAN in scar tissue
2	M	42	recurrent attacks of pain in the left parietotemporal and periauricular region for over two years, especially during sun exposure	slightly larger GAN on the symptomatic side during its whole course. US-guided block was successful	suspected neuritis of the GAN
3	M	41	patient suffered a fracture of the left clavicle. One day after trauma, he developed numbness of the left cheek and pain in the lateral head	distinct and extensive swelling of the GAN that could be followed until entering the parotid gland, identified as a traction neuroma	traction neuroma of the GAN
4	F	36	spontaneous development of continuous pain in the left ear and periauricular region	no obvious findings of GAN on affected side, pulsed radiofrequency was successful	neuropathic pain of the GAN of unknown origin
5	F	75	patient suffered recurrent carcinoma of the parotid gland and developed strong pain in the left retroauricular region that was exacerbated when turning the head	infiltration of the GAN by the tumorous mass	tumorous infiltration of the GAN
6	M	23	surgery for a cyst on the left lateral neck. Days after surgery, the patient developed pain within the innervation territory of the GAN	1.5 cm mass on the sternocleidomastoid muscle in continuity with the GAN, compatible with a stump neuroma	iatrogenic GAN transection
7	F	22	neurofibromatosis type I, onset of pain in the right ear and lateral head, spreading down to the supraclavicular fossa	multiple neurofibromas along cervical plexus, including the GAN	neurofibromatosis of the GAN

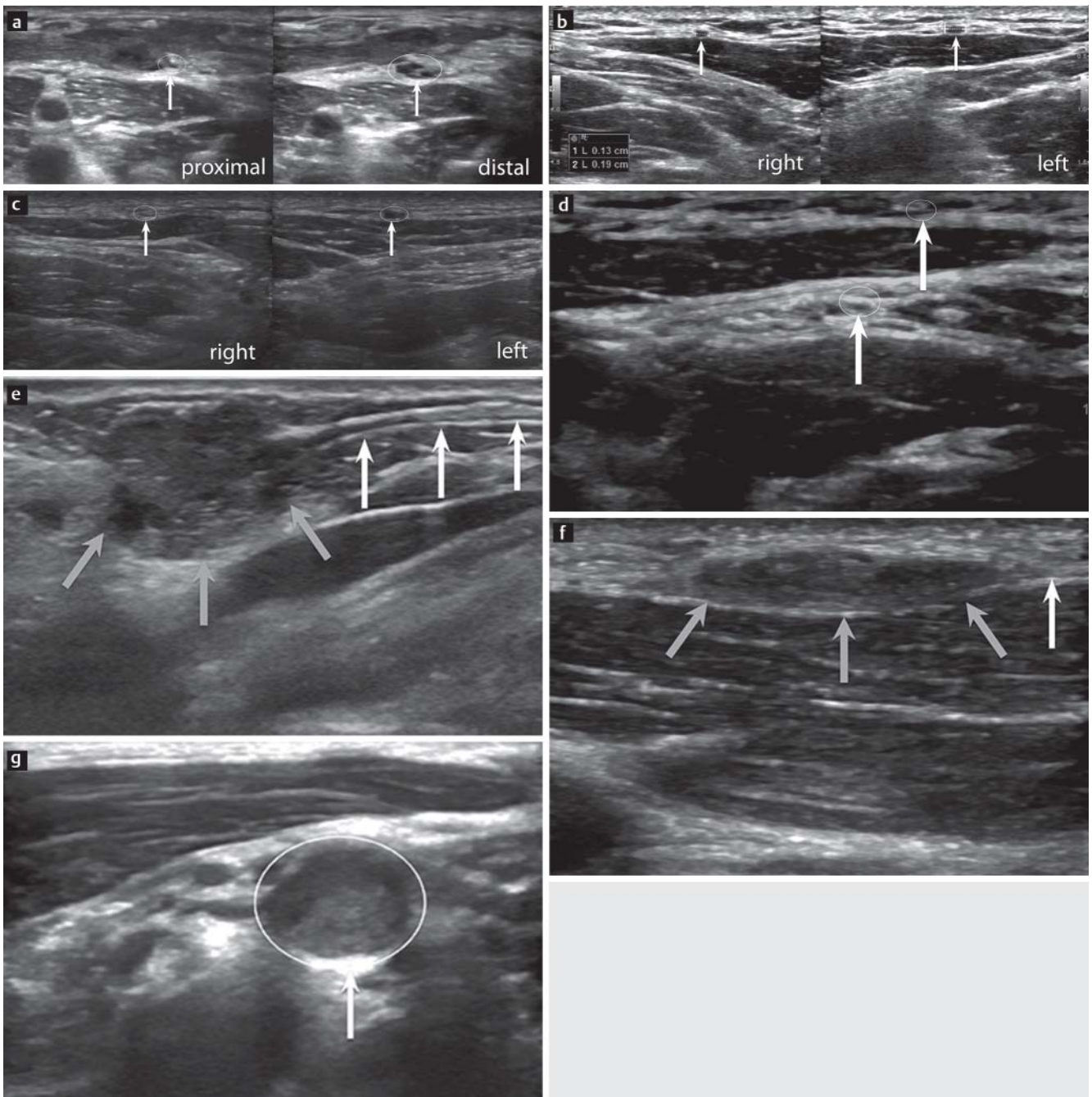


Fig. 4 **a** Findings in patient 1, showing an enlarged GAN proximally (both pictures on the left side). **b** Findings in patient 2, showing an enlarged GAN on the left side compared to the right. **c** Findings in patient 3, showing a traction neuroma of the GAN on the left side. **d** Findings in patient 4, showing normal findings on symptomatic side. **e** Findings in patient 5, showing the left GAN in longitudinal view (white arrows), as entering the tumorous mass (gray arrows). **f** Findings in patient 6, showing the left GAN in longitudinal view (white arrow), continuing with a stump neuroma (gray arrows). **g** Findings in patient 7, showing multiple neurofibromas within the superficial cervical plexus, white arrow pointing at GAN (additionally encircled).

Abb. 4 **a** Befund Patientin 1 mit einem verdickten GAN proximal (beide Bilder linke Seite). **b** Befund Patient 2 mit einem vergrößerten GAN links verglichen mit rechts. **c** Befund Patient 3: Traktionsneurom des GAN links. **d** Befund Patientin 4 mit unauffälligem GAN auf der symptomatischen Seite. **e** Befund Patientin 5: GAN longitudinal (weiße Pfeile) mit Eintritt in den Tumor (graue Pfeile). **f** Befund Patient 6 mit GAN longitudinal (weißer Pfeil) und Stumpfneurom im Verlauf (graue Pfeile) **g** Befund Patientin 7 mit multiplen Neurofibromen im Bereich des Plexus cervicalis superficialis (weißer Pfeil und eingekreist = GAN).

In all anatomical specimens the GAN (n = 12) was identified, ink marked and confirmed as successfully identified by dissection (● Fig. 3).

Its normal appearance is usually one hypoechoic, round dot in transverse view, with a small surrounding slightly hyperechoic border. The individual fascicles were not visible in the ma-

jority of cases with the 18 MHz high-resolution probe. The average nerve diameter in healthy volunteers was $0.14 \text{ cm} \pm 0.03$ (range 0.08 to 0.2) (● Table 1). The maximum detectable side difference was 0.03 cm.

The histories and HRUS findings for all patients in our department who were identified as having GAN pathologies are pres-

ented in [Table 2](#) and [Fig. 4a-g](#). This included one patient with a traumatic neuroma, one with a stump neuroma after surgery, one with compression of the GAN by scar tissue following surgery, one tumor infiltration, one patient with neurofibromatosis that affected the superficial cervical plexus including the GAN and two cases that were classified as idiopathic, as no triggers could be identified. These two cases included one patient, in whom a slight swelling of the GAN was suspected over most of its course and one patient whose GAN did not show any morphological alterations on HRUS. All cases – as mentioned above – underwent diagnostic selective blockade of the GAN for confirmation of pain origin within its territory.

Discussion

This study confirms the ability to reliably identify and evaluate the GAN with HRUS by ultrasound-guided ink marking and consecutive dissection in a series of anatomical specimens. We further present first measures of the GAN in healthy volunteers with a mean diameter of 1.4 mm and seven cases of GAN pathologies seen at our department, confirmed by selective GAN blockade, after which patients experienced complete symptom relief within minutes.

Following the rule of assessment for small, superficially running nerves – that a sweeping view is much better for detection than a static US image [20] – the GAN is rather easy to detect compared to other small nerves in this region. The posterior border of the sternocleidomastoid muscle as the main landmark is easily assessed clinically and also shows a distinct, drop-like shape on the transverse view. After identification, only a rather small area needs to be examined and, with some experience, the time required for assessment should not exceed 15 minutes for each side, including diagnostic and/or therapeutic blockade.

Concerning possible pathologies, there seems to be a rather broad spectrum that can be expected, including idiopathic, iatrogenic, traumatic or tumorous infiltration.

Two of our patients underwent surgery of the neck, which was followed by pain within the GAN territory. In the patient with entrapment of the GAN in scar tissue after neck dissection (Patient 1), resection may have been inevitable, as the GAN may also have been infiltrated. In the patient with iatrogenic transection of the GAN after surgery because of a neck cyst (Patient 6), however, the GAN could have been preserved. Neuromas after neck dissection were reported in 2.7% of the patients [21] and must be differentiated from recurrent lymphadenopathy, which was recently reported to be successfully achieved with sonography [22], thereby avoiding additional surgery. The literature suggests that neck surgery with the preservation of the GAN is preferable, whenever possible, as it does not result in a higher risk of disease recurrence in carcinomas [4, 5].

In the patient with traction trauma of the GAN (Patient 3), this seemed to have occurred when the clavicle was fractured, as HRUS showed a circumscribed traction neuroma at the point where the GAN winds around the posterior border of the sternocleidomastoid muscle. We suspect that this can happen when the head is forcefully turned to the other side and the ventral shoulder girdle is pulled downward.

Wherever present, HRUS can easily detect focal nerve pathology, such as neurofibromatosis of the GAN (Patient 5) or tumorous infiltration of the GAN (Patient 7).

However, two of the patients showed no obvious reason for GAN pathology (Patient 2 and Patient 4). They spontaneously developed pain, with no trauma-related injury. There were no abnormalities detectable in otorhinolaryngologic examination or of the skin of and around the outer ear. The HRUS findings also differed from the other patients in the group. One patient showed no swelling throughout the course of the GAN and the other had no segmental enlargement within the course, but a diffusely enlarged diameter compared to the contralateral side throughout the whole course of the GAN. The difference between sides was bigger than the variation observed in volunteers. However, to date, as we have no information about natural intra- and inter-individual variations in the nerve diameter of the GAN for the general population, this is only a hypothesis. Suspension of pain after selective blockade strengthens our idea that detectable differences in diameters between the two sides are meaningful. The pathogenesis of the nerve swelling was unclear in Patient 4. We are aware of one paper that dealt with an increased cross-sectional area in the major occipital nerve in patients with unilateral occipital neuralgia on the symptomatic side, compared to the asymptomatic side [18]. But, this was measured at only one point and no information was given about the remaining nerve. Also, the greater occipital nerve is at high risk for compression at no less than six points throughout its course [23], so this might well have been only a phenomenon caused by measurement next to a compression site.

In this study sample, patients with an idiopathic onset showed a different clinical presentation and did not describe neuralgia, but rather, constant pain. In addition, these patients showed pain distribution outside the GAN territory. Case 2, in particular, is therefore remarkable, as pain in the ear came with paraesthesias, as well as pain in the face and unilaterally on the head. We attribute this to the contribution of sensory C2 fibers to the trigemino-cervical complex in the brain stem [24], where nociceptive afferents from the trigeminal nerve and C1 to C3 converge, thus causing the phenomenon of referred pain, which is well known in headache patients. The patient with suspected neuritis of the GAN (Case 2) is also a cautionary signal, because the symptoms led to a questionable indication for the extraction of a tooth.

To conclude, we consider HRUS evaluation of the GAN a simple tool that should be applied whenever: (a) there is a history of trauma or surgery on the neck or upper thoracic aperture that is followed by pain in the lateral neck, head, and ear; and (b) whenever there is a clinically atypically presentation of unilateral headache, also involving the ear. As we saw seven patients within one year, we think that GAN pathology might be quite frequent, but not yet considered in the differential diagnosis.

References

- 1 *Becser N, Bovim G, Sjaastad O.* Extracranial nerves in the posterior part of the head. Anatomic variations and their possible clinical significance. *Spine (Phila Pa 1976)* 1998; 23: 1435–1441
- 2 *Standring S.* *Gray's Anatomy.* 40th ed. Churchill Livingstone Elsevier; 2008
- 3 *Sand T, Becser N.* Neurophysiological and anatomical variability of the greater auricular nerve. *Acta Neurol Scand* 1998; 98: 333–339
- 4 *George M, Karkos PD, Dwivedi RC et al.* Preservation of greater auricular nerve during parotidectomy: Sensation, quality of life, and morbidity issues. A Systematic Review. *Head Neck* 2013; DOI: 10.1002/hed.23292
- 5 *Li Y, Zhang J, Yang K.* Evaluation of the efficacy of a novel radical neck dissection preserving the external jugular vein, greater auricular

- nerve, and deep branches of the cervical nerve. *Onco Targets Ther* 2013; 6: 361–367. DOI: 10.2147/OTT.S43073
- 6 Herring AA, Stone MB, Frenkel O et al. The ultrasound-guided superficial cervical plexus block for anesthesia and analgesia in emergency care settings. *Am J Emerg Med* 2012; 30: 1263–1267. DOI: 10.1016/j.ajem.2011.06.023
 - 7 Selekler M, Kutlu A, Ucar S et al. Immediate response to greater auricular nerve blockade in red ear syndrome. *Cephalalgia* 2009; 29: 478–479. DOI: 10.1111/j.1468-2982.2008.01756.x
 - 8 Suresh S, Bellig G. Regional anesthesia in a very low-birth-weight neonate for a neurosurgical procedure. *Reg Anesth Pain Med* 2004; 29: 58–59
 - 9 Neopane A, Upadhyaya B, Dungana S et al. Study of patients presenting with symptoms of peripheral neuropathy and thickened greater auricular nerve. *Kathmandu Univ Med J (KUMJ)* 2003; 1: 3–7
 - 10 Lynch P. Greater auricular nerve in diagnosis of leprosy. *Br Med J* 1978; 2: 1340
 - 11 Ramesh V, Jain RK, Avninder S. Great auricular nerve involvement in leprosy: scope for misdiagnosis. *J Postgrad Med* 2007; 53: 253–254
 - 12 Ng AK, Page RS. Greater auricular nerve neuropraxia with beach chair positioning during shoulder surgery. *Int J Shoulder Surg* 2010; 4: 48–50. DOI: 10.4103/0973-6042.70824
 - 13 Park TS, Kim YS. Neuropraxia of the cutaneous nerve of the cervical plexus after shoulder arthroscopy. *Arthroscopy* 2005; 21: 631. DOI: 10.1016/j.arthro.2005.02.003
 - 14 Vorobeichik L, Fallucco MA, Hagan RR. Chronic daily headaches secondary to greater auricular and lesser occipital neuromas following endolymphatic shunt surgery. *BMJ Case Rep* 2012; DOI: 10.1136/bcr-2012-007189
 - 15 Tubbs RS, Salter EG, Wellons JC et al. Landmarks for the identification of the cutaneous nerves of the occiput and nuchal regions. *Clin Anat* 2007; 20: 235–238. DOI: 10.1002/ca.20297
 - 16 Christ S, Kaviani R, Rindfleisch F et al. Brief report: identification of the great auricular nerve by ultrasound imaging and transcutaneous nerve stimulation. *Anesth Analg* 2012; 114: 1128–1130. DOI: 10.1213/AN.E.0b013e3182468cc1
 - 17 Thallaj A, Marhofer P, Moriggl B et al. Great auricular nerve blockade using high resolution ultrasound: a volunteer study. *Anaesthesia* 2010; 65: 836–840. DOI: 10.1111/j.1365-2044.2010.06443.x
 - 18 Cho JC, Haun DW, Kettner NW. Sonographic evaluation of the greater occipital nerve in unilateral occipital neuralgia. *J Ultrasound Med* 2012; 31: 37–42
 - 19 Bodner G, Harpf C, Gardetto A et al. Ultrasonography of the accessory nerve: normal and pathologic findings in cadavers and patients with iatrogenic accessory nerve palsy. *J Ultrasound Med* 2002; 21: 1159–1163
 - 20 Bodner G, Bernathova M, Galiano K et al. Ultrasound of the lateral femoral cutaneous nerve: normal findings in a cadaver and in volunteers. *Reg Anesth Pain Med* 2009; 34: 265–268. DOI: 10.1097/AAP.0b013e31819a4fc6
 - 21 Iida S, Shirasuna K, Kogo M et al. Amputation neuroma following radical neck dissection—report of 3 cases. *J Osaka Univ Dent Sch* 1995; 35: 1–4
 - 22 Ha EJ, Baek JH, Lee JH et al. Characteristic ultrasound feature of traumatic neuromas after neck dissection: direct continuity with the cervical plexus. *Thyroid* 2012; 22: 820–826. DOI: 10.1089/thy.2012.0092
 - 23 Janis JE, Hatef DA, Ducic I et al. The anatomy of the greater occipital nerve: Part II. Compression point topography. *Plast Reconstr Surg* 2010; 126: 1563–1572. DOI: 10.1097/PRS.0b013e3181ef7f0c
 - 24 Busch V, Frese A, Bartsch T. The trigemino-cervical complex. Integration of peripheral and central pain mechanisms in primary headache syndromes. *Schmerz* 2004; 18: 404–410. DOI: 10.1007/s00482-004-0347-x